

Boehmite Nanoparticle-enhanced Jatropha Oil Nanofluid: Synthesis, Stability, and Viscosity Analysis

Surya Kumari Joshi^{1,2,3,4,5} Dinesh Kumar Chaudhary^{5,6}, Md Al-Mamun⁵, Sheikh Manjura Hoque⁵, Surya Prasad Adhikari⁷, Rabindra Prasad Dhakal⁸, Rameshwar Adhikari^{1,3,4}*

¹Central Department of Chemistry, Tribhuvan University, Kirtipur 44818, Kathmandu, Nepal

²Nepal Oil Corporation Limited, Babarmahal, Kathmandu, Nepal

³Research Centre for Applied Science and Technology (RECAST), Tribhuvan University, Kirtipur 44618, Kathmandu, Nepal

⁴Nepal Polymer Institute (NPI), P. O. Box 24411, Kathmandu, Nepal

⁵Material Science Division, Atomic Energy Centre Dhaka (AECD), Bangladesh

⁶Department of Physics, Amrit Campus, Tribhuvan University, Leknath Marg, Lainchour, Kathmandu 44600, Nepal

⁷Department of Mechanical and Aerospace Engineering, Pulchowk Campus, Tribhuvan University, Lalitpur, Kathmandu, Nepal

⁸Nepal Academy of Science and Technology (NAST), Khumaltar, Lalitpur, Nepal

*Corresponding E-mail: nepalpolymer@yahoo.com,

(Received: July 15, 2025, revised: July 25, 2025, accepted: August 5, 2025)

Abstract

The jatropha nanofluid (JNF) was prepared by blending jatropha oil (JO) with 0.1 wt.-% boehmite nanoparticles (B-NPs) and was subsequently characterized for its chemical composition, nanostructural stability, and flow properties using Fourier-transform infrared (FTIR) spectroscopy, zeta potential, and sedimentation tests, and a type B Ostwald viscometer, respectively. X-ray diffraction (XRD) analysis revealed the polycrystalline nature of boehmite with a crystallite size of 8.19 ± 0.57 nm, while Transmission electron microscopy (TEM) showed its platelet-like morphology. With a zeta potential value of 27.3 mV, the nanofluid was suggested to be moderately stable. The addition of B-NPs led to an increase in the kinematic viscosity of jatropha oil, attributed to the enhanced internal resistance caused by suspended nanoparticles. These nanoparticles alter the microstructure of the fluid and influence the formation of interaction layers and particle clusters. The observed enhancement in viscosity suggests that the B-NPs-modified jatropha oil holds potential as an environmentally friendly biolubricant or hydraulic fluid for mechanical applications.

Keywords: Nanofluid, Boehmite nanoparticle, Kinematic viscosity, Electron microscopy, Biolubricant

Introduction

Widely used in mechanical operations and known for playing vital roles in saving the lives of machines in manufacturing industries, a lubricant is a substance that reduces friction between mating surfaces and prevents the latter from being worn out [1-3]. Generally, the use of petroleum-based lubricants creates serious environmental risks and disposal challenges. Instead, traditional cutting fluids

can damage the operator's health by causing skin diseases, respiratory disorders, throat infections, and asthma [4, 5]. Thus, a new lubricant called a bio-lubricant (derived from animal fat and vegetable oil) is urgently needed, either as cutting fluids or other products, that exhibits superior lubricating behavior and is environmentally friendly [3,6]. The renewable sources, like vegetable oils, have enormous

potential to solve the problems mentioned above because of their good thermophysical and tribological qualities and lower toxicity [7, 8]. To improve the quality of vegetable oils, the researchers are trying to tune the thermophysical and tribological properties of vegetable oils by adding metal oxides and other nanoparticles (such as boehmite, copper oxide, boron nitride, etc.) to form a stable emulsion called a nanofluid [9]. Nanofluids based on various vegetable oils (like coconut, jatropha, canola, soybean, and peanut) are utilized as metal-cutting aids [8].

Among various additives in use, boehmite nanoparticles are potential candidates for bio-lubricating nanofluids with improved rheological and tribological properties [10]. It is known that boehmite is used as a precursor for preparing many aluminium-based compounds. It is specifically utilized to create cement catalysts, membranes, adsorbents, abrasives, composites, high-temperature ceramic coatings, and materials with photoluminescent properties [11-21]. In addition, boehmite demonstrated superior friction, wear, and extreme pressure reduction in comparison to the base oil, poly- α -olefin 6 (PAO-6) alone [10]. Uniformly distributed nanoparticles can enhance the thermophysical, rheological, and tribological properties of base fluids, making them suitable for use in cooling, power generation, and machining [22,23]. For example, Gobane and coworkers added the copper oxide nanoparticles (CuO) to jatropha oil (JO), created their nanofluids, and evaluated the thermal conductivity and viscosity. Nanofluids have been demonstrated to exhibit enhanced thermophysical properties [24]. Katpatal *et al.* reported further the enhancement in the thermal conductivity and viscosity of JO by the addition of CuO nanoparticles [25]. Talib et al. added the boron nitride NPs to the JO and found an increase in

wear resistance and trapping torque efficiency compared to the neat JO [26].

The literature survey reveals that JO derived from *Jatropha curcas* seeds is one of the biodegradable candidates for biolubricant formulation and holds significant importance for environmentally friendly and sustainable development. It has found widespread use in biodiesel production [27], but not much research has been conducted on its application in machining. As jatropha is easily accessible, cost-effective, non-edible, and practically harmless to the environment, this work is aimed at synthesizing the jatropha nanofluid and carrying out the first investigations towards its suitability for lubrication purposes.

Materials and Methods

Jatropha oil (JO) extracted by the cold press method was obtained from a local vegetable oil supplier from Dhangadhi, Nepal. The commercially available *p*-toluene sulfonic acid modified boehmite nanoparticles powder, AlO(OH), (commercial name: Disperal OS1), was provided by Sasol, Hamburg, Germany.

Production of jatropha nanofluid (JNF)

The nanofluid was prepared by mixing 0.1% (w/w) boehmite nanoparticles with JO, following the two steps. First, the nanoparticles and oil were blended under constant stirring at a temperature of 70 °C on a heating plate equipped with a magnetic stirrer for 1 h (**Figure 1(a)**). Next, the mixture solution was homogenized ultrasonically for 6 h, keeping the temperature below 50 °C, as shown in **Figure 1(b)**.

Analytical Techniques

X-ray diffraction (XRD) was performed using a Fast Detector X-ray Diffractometer (Smart Lab SE, Rigaku Corporation, Japan) with a K β filter 1D for Cu in the 2 θ range from 10~80 °having an X-Ray generator of 40 kV 40 mA, a step width of 0.02°, and a scan speed of 10°/min.

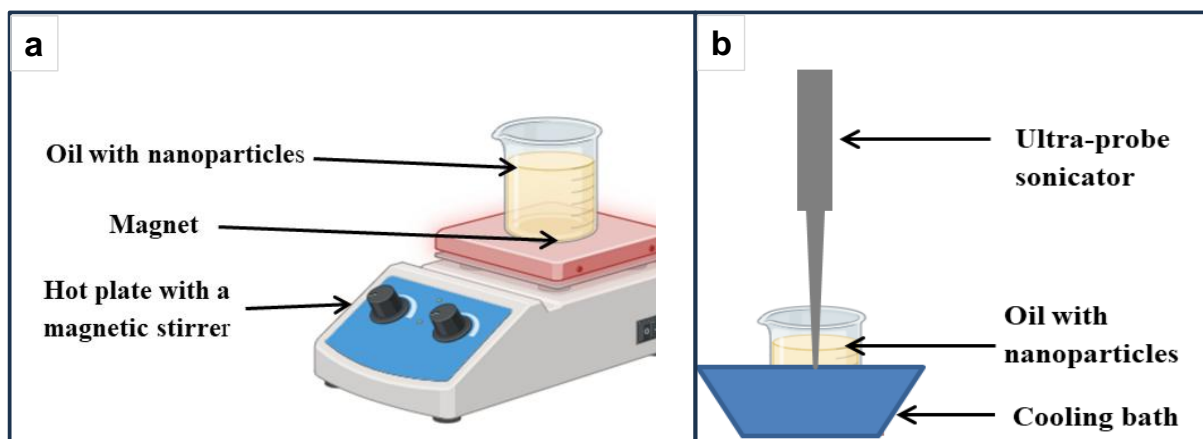


Figure 1: Schematic diagram showing the nanofluid preparation process. (a) a hot plate equipped with a magnetic stirrer, and (b) the process of ultrasonication of the mixture.

Energy-dispersive X-ray spectroscopy (EDX) (S50 QLD9111, FEI, Amsterdam, The Netherlands) was used for the elemental composition of the B-NPs.

A high-resolution Transmission Electron Microscope (TEM) equipped with energy electron loss spectroscopy (EELS) and accessories (TALOS F200 G2, USA) operating at an acceleration voltage of 200 kV was used to analyze the morphology of the B-NPs.

Fourier transform infrared (FTIR) spectroscopy (STA, 449 F3 Jupiter, UK) was exploited to resolve the functional group of B-NPs, JO, and JNF. The spectra were scanned at a resolution of 4 cm^{-1} and over the wavenumber range of $400\text{--}4000\text{ cm}^{-1}$.

Zeta Sizer (Nano ZS, UK) was applied to determine the zeta potential of JNF as well as the zeta size of the B-NPs in JNF.

Ostwald viscometer type B with both water and silicon oil baths was used to find the kinematic viscosity of JO and JNF.

Results and Discussion

Characterization of B-NPs

We first investigated the crystalline texture, size, and orientation of the B-NPs, followed by

their orientation to condensed phase morphology and elemental analysis. **Figure 2a** depicts the XRD pattern of B-NPs. Multiple peaks were observed at the 2θ values of 14.44° , 28.16° , 38.33° , 45.91° , 49.21° , 51.68° , 55.19° , 60.47° , 64.43° , 67.36° , and 71.98° , corresponding to (020), (021), (130), (131), (002), (151), (080), (132), (171), and (152) planes, respectively, indicating a polycrystalline nature of the B-NPs.

The observed peaks were well matched to the DB Card Number 01-073-9093 with space group Cmc m 63. The size of a crystallite was calculated by Debye-Scherrer's equation (i):

$$D = 0.9\lambda / \beta \cos\theta \quad \text{..... (i)}$$

where D = crystalline size, λ = the wavelength of the X-ray beam, β = full width of half maximum intensity peak expressed in radians, and θ = Bragg's diffraction angle.

The crystallite size of the B-NPs was calculated to be $8.19 \pm 0.57\text{ nm}$, having a crystal structure made up of an orthorhombic unit cell containing lattice parameters $a = 0.286522\text{ nm}$, $b = 1.223912\text{ nm}$, $c = 0.368863\text{ nm}$, and $\alpha^\circ = \beta^\circ = \gamma^\circ = 90^\circ$, which were similar to the results reported earlier by Jokanovi *et al* [28].

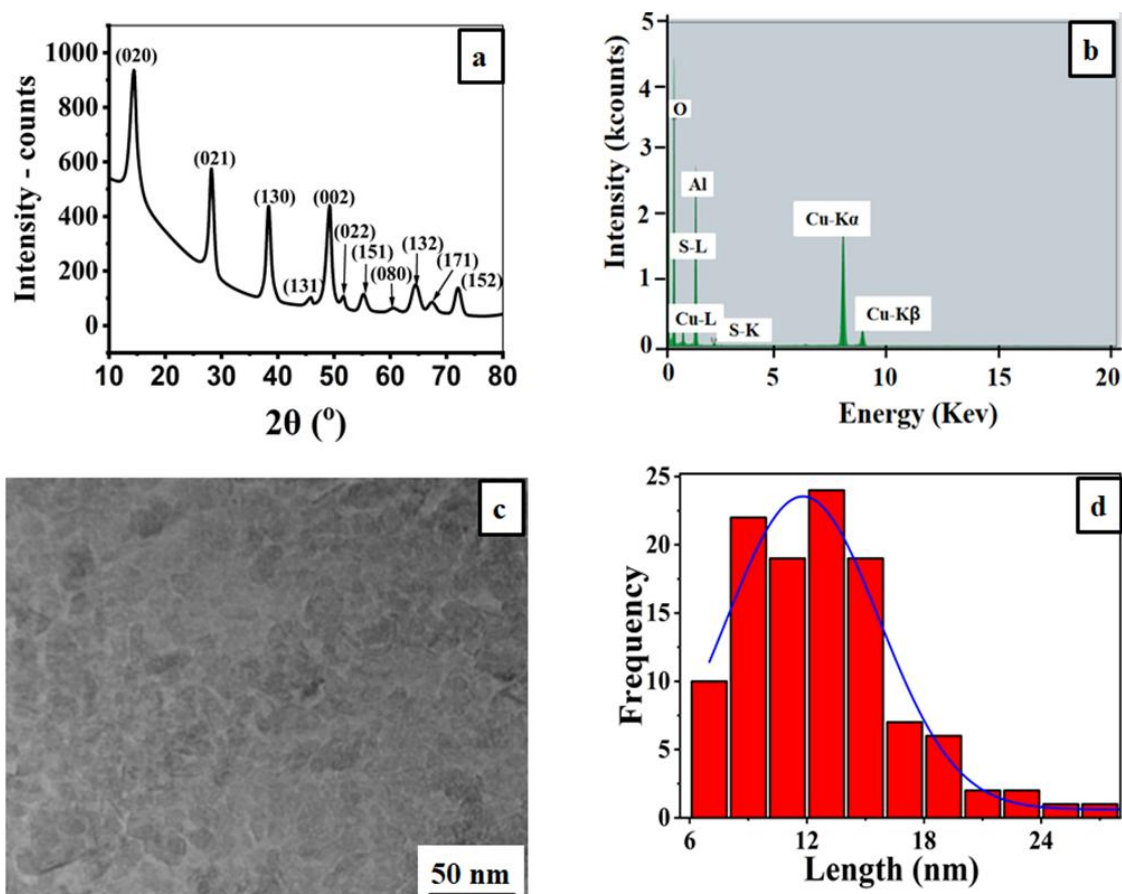


Figure 2: a) XRD pattern of boehmite powder (B-NPs), showing Miller indices corresponding to different crystal planes present; b) EDS of B-NPs; c) TEM image of boehmite nanoparticles, and d) size distribution of B-NPs calculated from TEM images

The EDS spectra of boehmite nanoparticles are presented in **Figure 2b**. The spectra of boehmite show that the sample contained C, O, Al, S, and Cu, having atomic fraction percentages of 42.11 ± 5.41 , 31.98 ± 7.61 , 13.62 ± 3.21 , 0.25 ± 0.06 , and 12.03 ± 2.22 , and mass fraction percentages of 12.03 ± 2.22 , 23.71 ± 5.08 , 17.04 ± 3.60 , 0.37 ± 0.08 , and 35.44 ± 5.42 , respectively. The presence of C and Cu may be due to the carbon-coated copper grids used as sample holders [29], and S, present in very small amounts, may be an impurity. The impurities, as indicated by the samples' EDS spectra, are, however, not evident in the XRD patterns.

In order to perform TEM analysis, the B-NPs were ultrasonically dispersed in ethanol and then dropped onto a carbon-coated copper grid. The TEM image of the sample is presented in **Figure 2c**, which shows the platelet-like

structure of the B-NPs. The average diameter of the B-NPs obtained from the TEM images was found to be 11.86 nm (see **Figure 2d**), quite close to the value suggested by the XRD. It is worth noting that discrepancies between the values obtained from the two techniques are inevitable, as TEM provides precise but localized information, whereas XRD offers averaged, bulk information about the material.

Characterization of the Jatropha Nanofluid

The nanofluid was analyzed by FTIR, zeta potential, and kinematic viscosity and viscosity index tests, which provide details about its functional groups, stability, and how easily it flows. The FTIR spectra (**Figure 3**) of the B-NPs show the absorption in the wavenumber range of $3000\text{--}3600\text{ cm}^{-1}$ corresponding to the stretching vibrations due to -OH groups, which might have originated from the loosely bound water molecules [30].

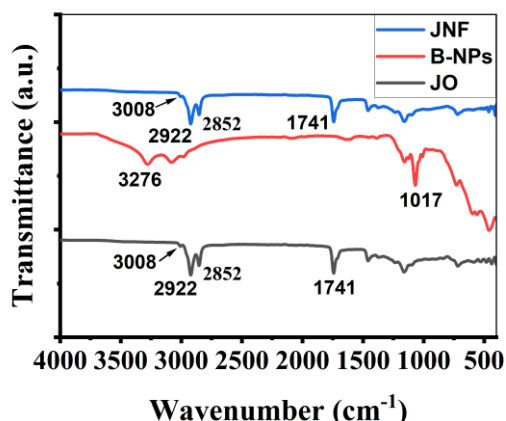


Figure 3: FTIR spectra of jatropha oil (JO), boehmite nanoparticles (B-NPs), and their nanofluid (JNF) as indicated.

Further, the Al-O-H bending mode in the region 900-1100 cm^{-1} confirmed the B-NPs [19]. Similarly, the presence of the peaks in the region 1680-1750 cm^{-1} implies the C=O stretching vibration of the carboxyl group, confirming the ester fatty acid in the JO. In JO, there are no clear peaks corresponding to -OH stretching, implying its purity with the absence of hydroxyl groups, neither from water nor from any other contaminants [31].

The FTIR bands indicated the existence of oleic acid, as indicated by the peaks centered at wavelengths of 2852 cm^{-1} , 2922 cm^{-1} , and 3007 cm^{-1} . Furthermore, the peaks observed in JNF resemble those in the JO. The reason behind this is due to the very low concentration of B-NPs dispersed in the oil. The low concentration of nanoparticles shows a too weak vibrational signal compared to the vegetable oil background, having a strong absorption band, as well as the fact that there is due to no significant bonding between the nanoparticles and the oil. As a result, there is no change in functional group, confirming the purely physical interaction between nanoparticles and the oil [32].

The stability of the nanofluid was determined by visual as well as zeta potential tests. When the nanofluid's stability was observed by visual test, no sedimentation was found within 3 months, which shows good

stability. For another stability test, a zeta potential analyzer was used to test the zeta potential of the nanofluid. It is noted that the value of zeta potential, either positive or negative, greater than 30, stands for good colloidal stability [33]. The results of the zeta potential measurements are presented in **Figure 4**.

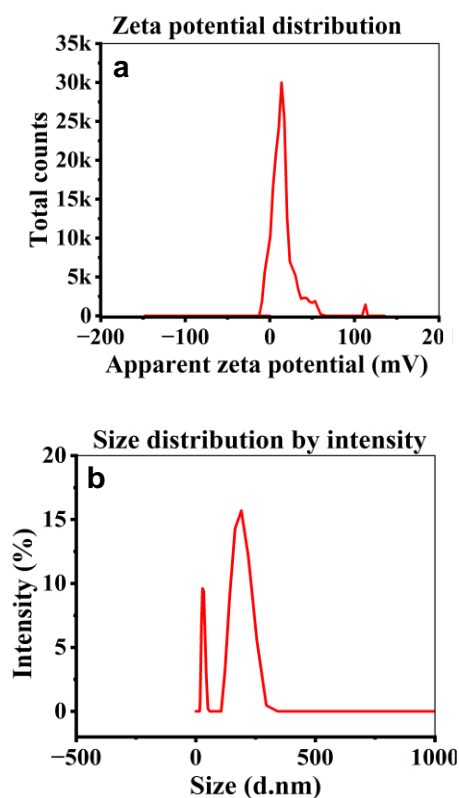


Figure 4: Zeta potential of JNF (a), and the hydrodynamic zeta size of B-NPs (b) in the fluid

It is observed that the zeta potential of the JNF was 27.3 mV (**Figure 4a**), having a zeta size of 163 nm (**Figure 4b**), which shows moderate stability. The stability of a nanofluid depends on the composition of fatty acids, the size of nanoparticles, and their compatibility with each other.

The nanofluid was stored in a dark place for several months, whereby no sedimentation was observed for 3 months, and the zeta potential remained 27.3 mV, demonstrating an excellent short-term colloidal stability, making the JNF a highly potential candidate for lubrication applications.

One of the most important factors influencing the lubricating oils' qualities and

effectiveness in a variety of applications is their kinematic viscosity (K.V.) [34, 35]. Low-viscosity materials flow easily, while high-viscosity materials flow very slowly. Fluid viscosity can be expressed in two different ways: kinematic viscosity and absolute (dynamic) viscosity [36]. Kinematic viscosity (K.V.), the foundation of viscosity index, is the ratio of absolute viscosity (expressed in centipoise, cP) to density (expressed in gcm^{-3}). It is expressed in centistokes (cSt) and accounts for the fluid density [36].

The K.V. of JO was 34.29 cSt, 17.85 cSt, 10 cSt, and 7.25 cSt at 40 °C, 60 °C, 80 °C, and 100 °C, whereas JNF's K.V. under similar conditions was 42.02 cSt, 21.79 cSt, 12.73 cSt, and 8.99 cSt, respectively. **Figure 5** shows the comparative bar diagram of the K.V. versus temperature of jatropha oil and its nanofluid. The JNF had a higher K.V. than neat oil, and it decreased as the temperature increased.

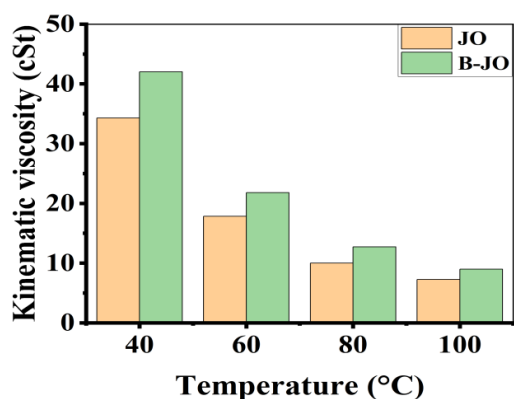


Figure 5: Kinematic viscosity of JO and B-JO at different temperatures as indicated.

In previous works, the aluminium oxide NPs were also added to coconut and jatropha oils to vary their viscosity in a controlled way, which is comparable to the outcome of the reported work [3, 37]. The reduction in oil viscosity at

elevated temperatures results from the increased molecular kinetic energy. The growing molecular kinetic energy caused more molecular collisions, thereby lessening the intermolecular interaction, which reduced the flow resistance and viscosity of a fluid at higher temperatures. In the case of a nanofluid, the elevated temperature increased the molecular vibration of the nanoparticles present in the nanofluid, which changed to the flow resistance of the fluid by affecting the microstructure and nature of interaction layers [38].

In the same way, another one of the popular matrices to evaluate the temperature-dependent flow characteristics of oil and lubricants is the viscosity index (V.I.), which shows the variation of viscosity of fluid with temperature [39-41]. For lubricating applications, a higher V.I. indicates greater viscosity stability at various temperatures. At low temperature with a high V.I., prevent noticeable thickening, allowing for rapid engine starting and effective oil flow. They also reduce oil consumption and ensure good lubrication by preventing severe thinning at high temperatures [42]. The viscosity index of JO and the JNF was 183 and 203, respectively, as determined by ASTM D2270. The K.V. measurements were conducted for this purpose at 40 °C and 100 °C [39, 43]. We observed that the JNF had an improved viscosity index after the addition of B-NPs. When the nanofluid was compared with ISO VG 46 [44], as shown in **Table 1**, lubricating properties like viscosity are comparable to each other, and the viscosity index is excellent, proving the importance of adding boehmite nanoparticles to the jatropha oil.

Table 1: Characterization of Jatropha nanofluid compared to ISO VG 46

Specification	Nanofluid (this work)	ISO VG 46	Testing Method
Kinematic viscosity cSt at 40 °C	42.02	>41.4	ASTM D 445
Kinematic viscosity cSt at 100 °C	8.99	>4.1	ASTM D445
Viscosity index	202.48	>90	ASTM D 2270

Instead of that, according to life cycle assessment (LCA) research, JO-based nanofluids are less harmful to the environment than the traditional cutting fluids [3]. Therefore, it can be used as a potential lubricant for short-term performance in future applications. For long-term performance, the JNF should be further stabilized by the addition of surfactants.

Conclusion

The B-NPs were characterized by X-ray diffraction (XRD), which confirmed their polycrystalline nature with an average crystallite size of 8.19 ± 0.57 nm. High-resolution transmission electron microscopy (TEM) revealed a platelet-like morphology. Energy-dispersive X-ray spectroscopy (EDS) indicated high purity of the boehmite, with only minor sulfur contamination, likely introduced during processing or nanoparticle preparation. A zeta potential value of 27.3 mV indicated that JNF was moderately stable. The addition of B-NPs resulted in a significant increase in the K.V. of JO, by approximately 22.54%, 22%, 27.3%, and 24% at temperatures of 40 °C, 60 °C, 80 °C, and 100 °C, respectively. This enhancement is attributed to an increase in internal resistance from the suspended nanoparticles, which alter the fluid's microstructure, interaction layers, and clusters. The improved K.V. and V.I. results of the JNF highlight a promising approach for enhancing lubricant performance, contributing to extended machine life. Furthermore, K.V. of JNF is comparable to ISO VG 46, indicating that the nanofluid meets the requirements for use as a hydraulic oil and may be utilized as a potential eco-friendly biolubricant.

Acknowledgements

SKJ sincerely thanks the Nepal Oil Corporation Limited for providing her with the study leave and providing the research facilities at its Central Laboratory, Sinamangal. The fellowship awarded to Ms. Surya Kumari Joshi by the International Science Programme, Uppsala University, Sweden, to conduct

research work at the Materials Science Division, Atomic Energy Centre, Dhaka, Bangladesh, under the program BAN:02/2, is gratefully acknowledged. We thank Ms. Deepshikha Karki (RECAST, Tribhuvan University) for critically reading the manuscript and Mr. Sadip Nepal (Department of Physics, Amrit campus, Tribhuvan University) for supporting in particle size distribution calculation from the TEM images.

Author's contribution statement

S. K. Joshi: Writing: original draft, formal analysis; **D. K. Chaudhary:** Writing: Co-drafting of manuscript, and XRD data analysis; **M. A. Mamun:** Validation and zeta potential analysis; **S. M. Hoque:** Validation, formal analysis, supervision, resources; **S. P. Adhikari:** Validation, writing: review & editing, and supervision; **R. P. Dhakal:** Validation, resources, investigation; **R. Adhikari:** Conceptualization, writing: review & editing, co-drafting of manuscript, resources, supervision.

Conflict of interest

The authors declare that they have no known competing financial interests or personal relationships that could have appeared to influence the work reported in this paper.

Data availability statement

Data will be provided on request.

References

1. K. J. Anderson, A History of Lubricants. MRS Bulletin, 1991, 16(10), 69–69. (DOI: 10.1557/S0883769400055895)
2. E. Abd Rahim, and H. Dorairaju, Evaluation of mist flow characteristic and performance in minimum quantity lubrication (MQL) machining. Measurement, 2018, 123, 213–225
DOI:10.1016/j.measurement.2018.03.015)
3. R. Singh, N. K. Sah, and V. Sharma,. Development and characterization of unitary and hybrid Al₂O₃ and ZrO dispersed Jatropha oil-based nanofluid for cleaner production, *Journal of Cleaner Production*, 2021, 317, 128365.

- (DOI:10.1016/j.jclepro.2021.128365)
4. P. Sharma, B. S. Sidhu, and J. Sharma, Investigation of effects of nanofluids on turning of AISI D2 steel using minimum quantity lubrication. *Journal of Cleaner Production*, 2015, 108, 72–79. (DOI:10.1016/j.jclepro.2015.07.122)
5. A. K. Singh, A. Kumar, V. Sharma, and P. Kala, Sustainable techniques in grinding: State of the art review, *Journal of Cleaner Production*, 2020, 269, 121876. (DOI:10.1016/j.jclepro.2020.121876)
6. S. Gariani, I. Shyha, F. Inam, and D. Huo, Experimental analysis of system parameters for minimum cutting fluid consumption when machining Ti-6Al-4V using a novel supply system. *The International Journal of Advanced Manufacturing Technology*, 2018, 95(5–8), 2795–2809. (DOI: 10.1007/s00170-017-1216-y)
7. M. Osama, A. Singh, R. Walvekar, M. Khalid, T. C. S. M. Gupta, and W. W. Yin, Recent developments and performance review of metal working fluids, *Tribology International*, 2017, 114, 389–401. (DOI:10.1016/j.triboint.2017.04.050)
8. A. S. A. Sani, E. Abd Rahim, S. Sharif, and H. Sasahara, The influence of modified vegetable oils on tool failure mode and wear mechanisms when turning AISI 1045. *Tribology International*, 2019, 129, 347–362. (DOI:10.1016/j.triboint.2018.08.038)
9. K. Lee, Y. Hwang, S. Cheong, Y. Choi, L. Kwon, J. Lee, and S. H. Kim, Understanding the role of nanoparticles in nano-oil lubrication, *Tribology Letters*, 2009, 35, 127–131. DOI: 10.1007/s11249-009-9441-7)
10. U. Maurya, and V. Vasu, Boehmite nanoparticles for potential enhancement of tribological performance of lubricants, *Wear*, 2022, 498, 204311. (DOI:10.1016/j.wear.2022.204311)
11. A. Alemi, Z. Hosseinpour, M. Dolatyari, and A. Bakhtiari, Boehmite (γ -AlOOH) nanoparticles: Hydrothermal synthesis, characterization, pH-controlled morphologies, optical properties, and DFT calculations. *Physica Status Solidi (b)*, 2012, 249(6), 1264–1270. (DOI:10.1002/pssb.201147484).
12. F. Granados-Correa, N. G. Corral-Capulin, M. T. Olguín, and C. E. Acosta-León, . Comparison of the Cd(II) adsorption processes between boehmite (γ -AlOOH) and goethite (α -FeOOH). *Chemical Engineering Journal*, 2011, 171(3), 1027–1034. (DOI:10.1016/j.cej.2011.04.055).
13. F. Granados-Correa, and J. Jiménez-Becerril, Chromium (VI) adsorption on boehmite, *Journal of Hazardous Materials*, 2009, 162(2–3), 1178–1184. (DOI:10.1016/j.jhazmat.2008.06.002).
14. K.-T. Hwang, H.-S. Lee, S.-H. Lee, K.-C. Chung, S.-S. Park, and J.-H. Lee, Synthesis of aluminium hydrates by a precipitation method and their use in coatings for ceramic membranes. *Journal of the European Ceramic Society*, 2001, 21(3), 375–380. (DOI: 10.1016/S0955-2219(00)00209-0).
15. B. Kindl, Y. L. Liu, E. Nyberg, and N. Hansen, The control of interface and microstructure of SiC/Al composites by sol-gel techniques. *Composites Science and Technology*, 1992, 43(1), 85–93. (DOI: 10.1016/0266-3538(92)90135-p).
16. B. Kindl, D. J. Carlsson, Y. Deslandes, and J. M. A. Hoddenbagh, Preparation of -Alumina Ceramics: The Use of Boehmite Sols as Dispersing Agents, *Ceramics International*, 1991, 17, 347–350. (DOI:10.1016/0272-8842(91)90032-U)
17. A. B. Kiss, G. Keresztury, and L. Farkas, Raman and ir spectra and structure of boehmite (γ -AlOOH): Evidence for the recently discarded D172h space group, *Spectrochimica Acta Part A: Molecular Spectroscopy*, 1980, 36(7), 653–658. (DOI: 10.1016/0584-8539(80)80024-9)
18. X. Lu, R. Zhu, and Y. He, Electrodeposited thin oxide films, *Surface and Coatings Technology*, 1996, 79(1–3), 19–24. (DOI: 10.1016/0257-8972(95)02456-5)
19. F. Ogata, N. Kawasaki, T. Nakamura, and S. Tanada, Removal of arsenious ion by calcined aluminum oxyhydroxide (boehmite), *Journal of Colloid and Interface Science*, 2006, 300(1), 88–93. (DOI:10.1016/j.jcis.2006.03.026).
20. G. K. Priya, P. Padmaja, K. G. K. Warriar, A. D. Damodaran, and G. Aruldas, Dehydroxylation and high temperature phase formation in sol+gel boehmite characterized by Fourier transform

- infrared spectroscopy, *Journal of Materials Science Letters*, 1997, 16, 1584–1587. (DOI:https://doi.org/10.1023/A:1018568418302)
22. N. K. Sah, R. Singh, and V. Sharma, Experimental investigations into thermophysical, wettability and tribological characteristics of ionic liquid based metal cutting fluids, *Journal of Manufacturing Processes*, 2021, 65, 190–205. (DOI:10.1016/j.jmapro.2021.03.019).
21. W.-H. Shih, L.-L. Pwu, and A. A. Tseng, Boehmite coating as a consolidation and forming aid in aqueous silicon nitride processing, *Journal of the American Ceramic Society*, 1995, 78(5). (DOI:10.1111/j.1151-2916.1995.tb08478.x)
22. J. P. Ajithkumar, and M. A. Xavier, Influence of nano lubrication in machining operations-a review. *Materials Today: Proceedings*, 2018, 5(5), 11185–11192. DOI:10.1016/j.matpr.2018.01.142)
24. S., T. Dama, N. Hasan, and E. Yanmaz, Characterization of Copper Oxide–Jatropha Oil Nanofluid as a Secondary Refrigerant, *Journal of Nanomaterials*, 2023, 2023, 1–7. (DOI:10.1155/2023/7612959).
25. D. C. Katpatal, A. B. Andhare, P. M. Padole, and R. S. Khedkar, Study of dispersion stability and thermo-physical properties of CuO–Jatropha oil-based nanolubricants, *Journal of the Brazilian Society of Mechanical Sciences and Engineering*, 2017, 39(9), 3657–3668. (DOI: 10.1007/s40430-017-0856-z).
26. N. Talib, R. M. Nasir, and E. A. Rahim, Tribological behaviour of modified jatropha oil by mixing hexagonal boron nitride nanoparticles as a bio-based lubricant for machining processes, *Journal of Cleaner Production*, 2017, 147, 360–378. (DOI:10.1016/j.jclepro.2017.01.086).
27. A. A. Abdelmalik, P. A. Abolaji, and H. A. Sadiq, Assessment of jatropha oil as insulating fluid for power transformers, *Journal of Physical Science*, 2018, 29(1), 1–16 (DOI:10.21315/jps2018.29.1.1)
28. V. Jekanovi, B. Jekanovi, B. Markovi, and Z. Markovi, Synthesis and characterization of hydrothermally obtained colloidal pseudo-boehmite/boehmite, *Journal of Optoelectronics and Advanced materials*, 2009, 11(2), 164–168.
29. M. Moreaud, D. Jeulin, V. Morard, and R. Revel, TEM image analysis and modelling: Application to boehmite nanoparticles, *Journal of Microscopy*, 2012, 245(2), 186–199. (DOI:10.1111/j.1365-2818.2011.03560.x)
30. W. Brostow, and T. Datashvili, Chemical modification and characterization of boehmite particles, *Chemistry and Chemical Technology*, 2008, 2(1), 27–32. (DOI:10.23939/chcht02.01.027)
31. M. Jayagobi, A. H. Alpandi, and H. Husin, Characterization of malaysian jatropha seed oil using ftir and gcms. Platform: A *Journal of Engineering*, 2021, 5(4), 23. (DOI: 10.61762/pajevol5iss4art15266).
32. I. Z. Luna, S. Chowdhury, M. A. Gafur, N. Khan, and Khan, A. Ruhul, Preparation and Characterization of CuO-PVA Nanofluids for Heat Transfer Applications. *Journal of Chemical Engineering and Chemistry Research*, 2015, 2(5), 607–615.
33. N. R. Pawar, M. Pawar, R. D. Chavhan, and O. P. Chimankar, Synthesis and spectroscopic characterization of Boehmite nanoparticles and its thermodynamic study, *Journal of Pure and Applied*, 2020, 42, 59–65.
34. B. Tormos, V. Bermúdez, S. Ruiz, and J. Alvis-Sanchez, Degradation effects of base oils after thermal and electrical aging for EV thermal fluid applications, *Lubricants*, 2023, 11(6), 241. (DOI: 10.3390/lubricants11060241)
35. Ł. Gierz, K. Perz, B. Wieczorek, C. Peixoto Matos, and Ł. Warguła, Kinematic Viscosity of Engine, Gear, Hydraulic and Special Purpose Oils at Temperatures of 25 C and 50 C, *Editorial Board of the Journal*, 3, 11–17. (DOI: 10.52209/2706-77X_2024_3_11)
36. L. N. Okoro, S. V. Belaboh, N. R. Edoeye, and B. Y. Makama, Synthesis, calorimetric and viscometric study of groundnut oil biodiesel and blends, *Synthesis*, 2011, 1, 3.
37. S. V. Sujith, A. K. Solanki, and R. S. Mulik, Experimental evaluation on rheological behavior

- of Al₂O₃-pure coconut oil nanofluids, *Journal of Molecular Liquids*, 2019, 286, 110905.
(DOI:10.1016/j.molliq.2019.110905)
38. M. Nabeel Rashin, and J. Hemalatha, Synthesis and viscosity studies of novel ecofriendly ZnO-coconut oil nanofluid, *Experimental Thermal and Fluid Science*, 2013, 51, 312–318.
(DOI:10.1016/j.expthermflusci.2013.08.014)
39. I. Stanciu, Viscosity index for oil used as biodegradable lubricant, *Indian Journal of Science and Technology*, 2020, 13(3), 352-359.
(DOI: 10.17485/ijst/2020/v13i03/147759)
40. A. A. A. Abdel-Azim, and R. M. Abdel-Aziem, Polymeric additives for improving the flow properties and viscosity index of lubricating oils, *Journal of Polymer Research*, 2001,8, 111-118.
(DOI: 10.1007/s10965-006-0140-x)
41. A. M. Nassar, Synthesis and evaluation of viscosity index improvers and pour point depressant for lube oil, *Petroleum Science and Technology*, 2008, 26(5), 523-531.
(DOI: 10.1080/10916460600809519)
42. A. Saka, T. K. Abor, A. C. Okafor, and M. U. Okoronkwo, Thermo-rheological and tribological properties of low-and high-oleic vegetable oils as sustainable bio-based lubricants, *RSC Sustainability*, 2025, 3(3), 1461-1476.
(DOI: 10.1039/D4SU00605D)
43. ASTM, D. Standard practice for calculating viscosity index from kinematic viscosity at 40 and 100° C, *Annual Book of Standards*, 2016.
44. E. K. Heikal, M. S. Elmelawy, S. A. Khalil, and N. M. Elbasuny, Manufacturing of environment friendly biolubricants from vegetable oils. *Egyptian Journal of Petroleum*, 2017, 26(1), 53–59.
(DOI: 10.1016/j.ejpe.2016.03.003)